3D Hybrid Modelling of Vascular Network Formation

Holger Perfahl[1,*], Barry D. Hughes[2], Tomás Alarcón[3,4,5], Philip K. Maini[6], Mark C. Lloyd[7], Matthias Reuss[1], Helen M. Byrne[6]

1 Center Systems Biology, University of Stuttgart, Stuttgart, Germany

2 School of Mathematics and Statistics, University of Melbourne, Australia

3 ICREA, Pg. Lluís Companys 23, 08010 Barcelona, Spain

4 Centre de Recerca Matemàtica, Campus de Bellaterra, Barcelona, Spain

5 Departament de Matemàtiques, Universitat Autònoma de Barcelona, Barcelona, Spain

6 Wolfson Centre for Mathematical Biology, Mathematical Institute, University of Oxford, Oxford, UK

7 H. Lee Moffitt Cancer Center and Research Institute, Tampa, USA

∗ **E-mail: holger.perfahl@ibvt.uni-stuttgart.de**

Supplementary Material

The Supplementary Material comprises three sections in which we describe the computational algorithm and parameter values that were used to generate the numerical results (S.1 and S.2, respectively), before presenting additional simulation results (S.3). Equation numbers in the following sections refer to the main text.

S.1 The Computational Algorithm

We now outline the algorithm that is used to generate numerical simulations of our hybrid, agent-based model (see, also, Figure S.1). We consider a three-dimensional Cartesian domain, of size $W_X \times W_Y \times W_Z$, discretised uniformly, with spacings ΔX, ΔY and ΔZ in the x, y and z directions, respectively. While an off-lattice approach is used to model the evolution of the vascular network, the domain discretisation is used to sort the cells (to increase computational efficacy in finding interacting neighbours [1]) and, thereby, to increase the speed of the numerical simulations. As stated above, the total number of segments (both tip and vessel segments) at time t is denoted by $N = N(t)$. The vascular network structure is stored

[1] Green S.,*Particle simulation using CUDA*, 2012, `http://docs.nvidia.com/cuda/samples/5_Simulations/particles/doc/particles.pdf`

in an undirected graph in which cell centre coordinates $\mathcal{N}$ and cell-cell connections $\mathcal{E}$ are recorded. The adjacency matrix $\mathcal{E}$ contains 2-tuples of the node numbers of all connections in the vessel network.

1. **Initialise the simulation ($t = 0$)**

   The initial network is defined by specifying a fixed number of vessels, the number of segments within each vessel, their positions and connectivity. Unless otherwise stated, the initial network comprises two parallel vessels, each formed of three elements (tip-vessel-tip). The initial cell cycle phase of each vessel element and the chemoattractant gradient are also prescribed ($\nabla c = (-c_x, 0, 0)$).

2. **Increment time ($t \to t + \Delta t$) and loop over all cells ($i = 1, \ldots, N(t)$)**

   The following steps are performed for each element in the network.

   (a) **Test for cell proliferation (vessel elements only)**

   If element i is a vessel element and $\phi_i \geq 1$ then it proliferates and its daughter cell is placed at a random position within a sphere of radius R_c centred on the parent cell. The daughter cell forms a new capillary sprout if its location is such that inequalities (10) are satisfied; otherwise, it becomes a vessel cell and contributes to elongation of the parent vessel.

   (b) **Update the position of element i**

   Different forces act on vessel and tip cells (see Equations (1) and (2)). We assume that these forces act on two different time-scales: a slow time-scale is associated with chemotactic and random movement, and a faster one with mechanically induced cell movement. We exploit this separation of time-scales by using a two-step method to integrate the equations of motion and update $\boldsymbol{x}_i$, the position of element i.

   - **Step 1.** Calculate the random force $\boldsymbol{F}_i^r$ using Equation (4). If cell i is a tip-cell, then calculate the chemotactic and persistence forces $\boldsymbol{F}_i^c$ and $\boldsymbol{F}_i^p$ using Equations (5) and (6). Update $\boldsymbol{x}_i$, the position of cell i, using an explicit Eulerian method to integrate Equation (1) for tip cells or (2) for vessel cells, and neglecting the mechanical and angular persistence forces.
   - **Step 2.** Calculate the mechanical force $\boldsymbol{F}_i^m$ using Equation (3) and if cell i is a vessel cell then calculate the angular persistence force $\boldsymbol{F}_i^a$ using Equation (7). If element i is a new cell, then its spring constant is increased in increments of $0.1S_c$ on consecutive time steps until it reaches the value S_c. Then $\boldsymbol{x}_i$, the position of cell i, is updated using an explicit

Eulerian method to integrate Equation (1) for tip cells or (2) for vessel cells. This step is repeated until the displacement on consecutive steps is less than a threshold ε or the number of iterations has reached the maximum value, $\max_{\text{iter}}$.

(c) **Update the cell cycle phase of cell i using Equation (8) (vessel elements only)**

(d) **Update vessel connectivity**

New connections are added to the vascular graph, and old ones removed when tip cells anastamose with other vessel segments or detach from their branch (detachment occurs if a tip-cell moves beyond the cut-off distance l_c, see Equation (3)).

3. If $t \geq T$ then end the simulation; otherwise, return to step 2.

A flowchart of the computational algorithm is given in Figure S.1. The algorithm illustrates how other species (e.g. normal cells, tumour cells, immune cells and tissue matrix) could be incorporated into the computational framework. We remark further that the order in which the algorithmic steps are carried out is arbitrary; reordering generates identical, mean results (results not included).

S.2 The Default Parameter Values

In the table that follows we state the default parameter values that were used to generate the numerical simulations. We stress that these parameter values were chosen to generate physically realistic results and not by fitting the model to experimental data (an investigation is beyond the scope of the current work).

S.3 Additional Simulation Results

In this section, we include additional simulation results Figures S.2–S.7 that complement those presented in the main text.

Table S.1. Summary of the parameters used in the computational model of vasculogenesis, along with their physical meaning and estimates of their dimensionless values (lengths are scaled with μm and times with sec).

Parameter	Physical meaning	Default value
R_c	target cell radius	5
l_c	cell interaction radius	$3R_c$
μ	drag coefficient	1
σ	sensitivity to random fluctuations	0.4
S_c	spring constant for compressed cells	5.56×10^{-6}
$100S_c$	spring constant for stretched cells	5.56×10^{-4}
χ	chemotactic sensitivity	0.1
c_x	chemoattractant gradient	5.56×10^{-4}
w_p	directional persistence coefficient	0.4
τ	directional persistence time	180
ω_a	angular persistence spring constant	5.56×10^{-5}
k_ϕ	progression rate through the cell cycle	1.39×10^{-5}
β_ϕ	cell cycle progression sensitivity to cell elongation and compression	100.0
k_{spr}	probability of sprouting	2.0×10^{-4}
K_{spr}	parameter for sprouting probability	0.01
W_X	domain length ($x-$direction)	1000
W_Y	domain length ($y-$direction)	1000
W_Z	domain length ($z-$direction)	1000
ΔX	grid spacing ($x-$direction)	20
ΔY	grid spacing ($y-$direction)	20
ΔZ	grid spacing ($z-$direction)	20
Δt	time step	180
$\max_{\text{iter}}$	max. number of iter. for calculation of tissue deformation per time step	10

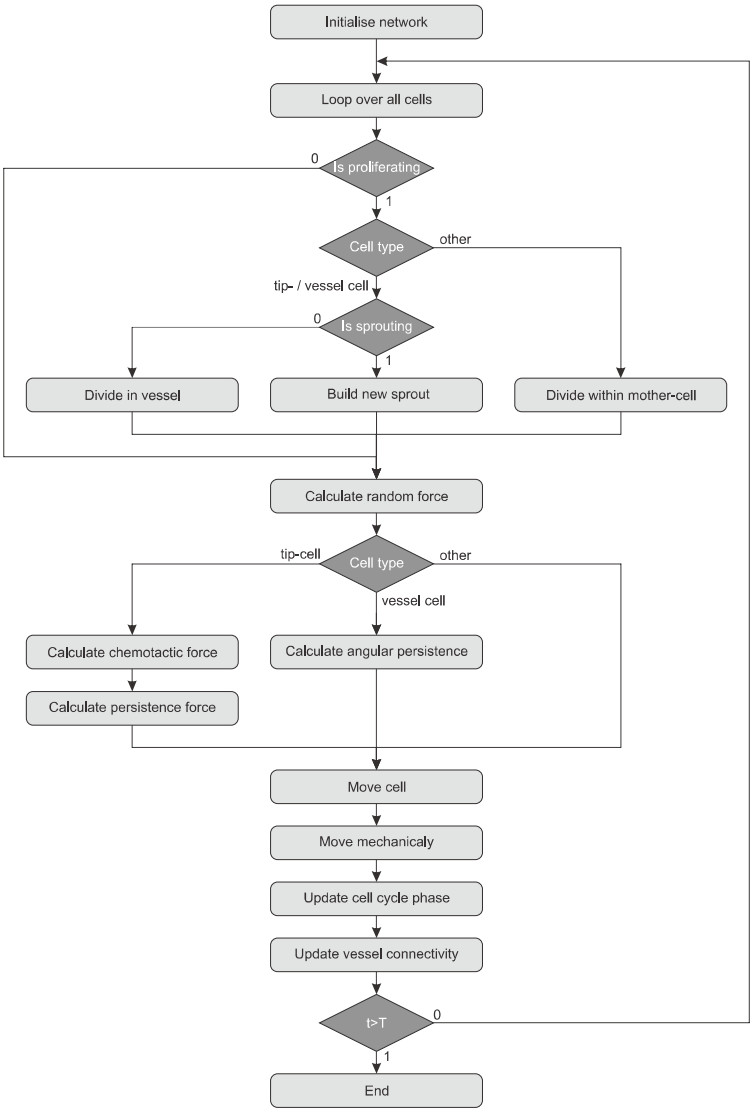

Figure S.1. Computational algorithm. This figure shows the computational algorithm used to simulate the off-lattice model of vasculogenesis.

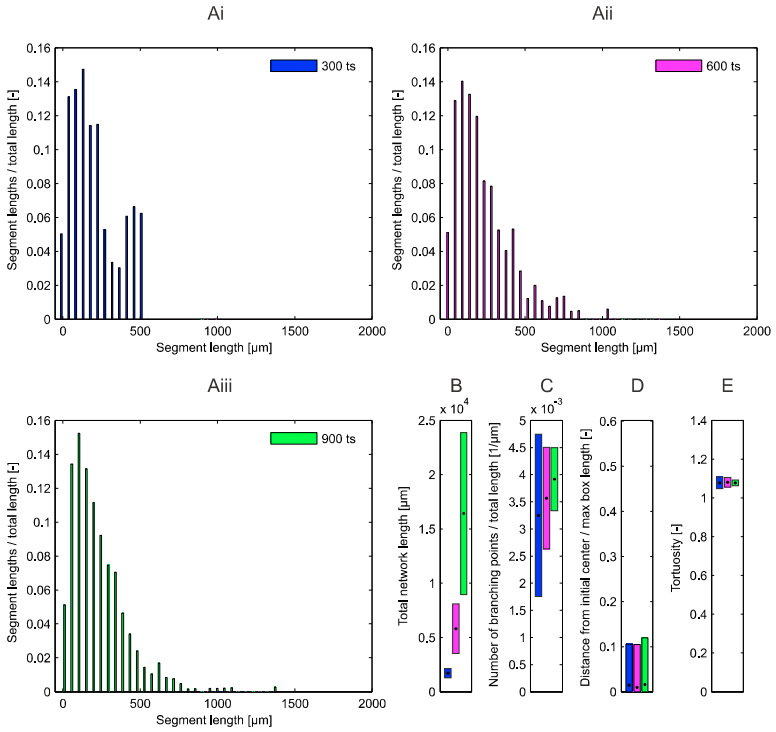

Figure S.2. Analysis of temporal network evolution. The metrics stabilise over time, while the total network length grows exponentially. **(Ai–iii)** the distribution of vessel lengths for $t = 300, 600, 900$ ts, **(B)** the total network length, **(C)** the number of branches per unit length; **(D)**, the displacement of the centre of mass, **(E)** the tortuousity. Key: in **(B)**–**(D)**, means illustrated by dots and standard deviations illustrated by bars were obtained by averaging over 70 simulations. Parameter values: as per Table S.1, except that the chemotactic sensitivity of the tip cells is $\chi = 0.0$.

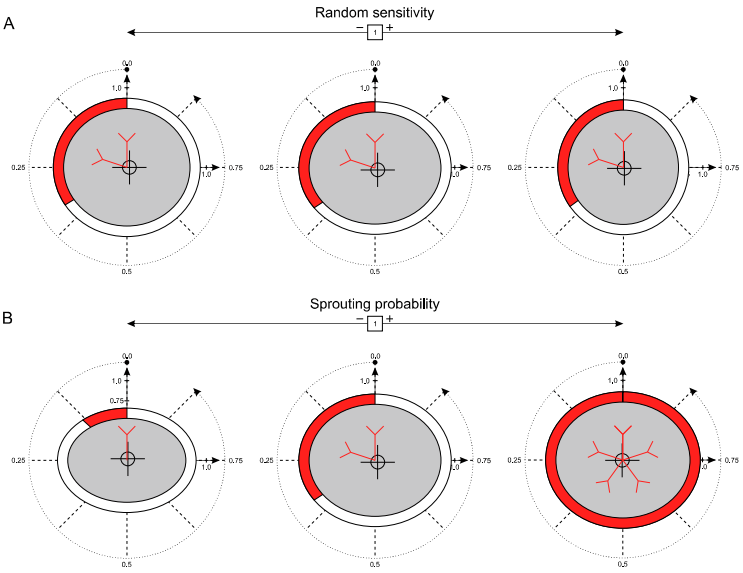

Figure S.3. Series of glyphs showing how the network metrics at time $t = 900\,\text{ts}$ depend on the strength of random sensitivity force and the sprouting probability. Each glyph represents the mean of 70 simulations at time $t = 900\,\text{ts}$. **(A)** the mean behaviour of the networks is does not change as the strength of the random motility force σ varies; **(B)** the total network length and the average number of branches per unit vessel length increase as the sprouting probability k_{spr} increases. For an explanation of the glyphs, see Figure 5. Parameter values: as per Table S.1, except $\chi = 0$ and (A) $\sigma = 0.2, 0.4, 0.8$ and $k_{\text{spr}} = 2.0 \times 10^{-4}$; (B) $k_{\text{spr}} = 1.0 \times 10^{-4}, 2.0 \times 10^{-4}, 4 \times 10^{-4}$ and $\sigma = 0.4$.

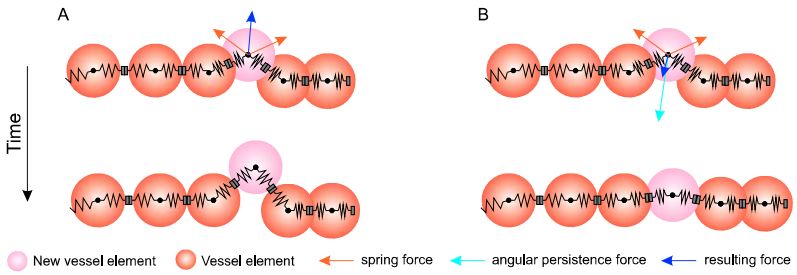

Figure S.4. The stabilising effect of the angular persistence force on vessel morphology. This figure illustrates how the angular persistence force stabilises vessel morphology after cell proliferation. **(A)** The new vessel element is pushed out of the vessel if the angular persistence force is neglected. **(B)** when active, the angular persistence force (see Equation (7)) prevents the new element from being pushed outwards from the parent vessel, leading, instead, to elongation of that vessel.

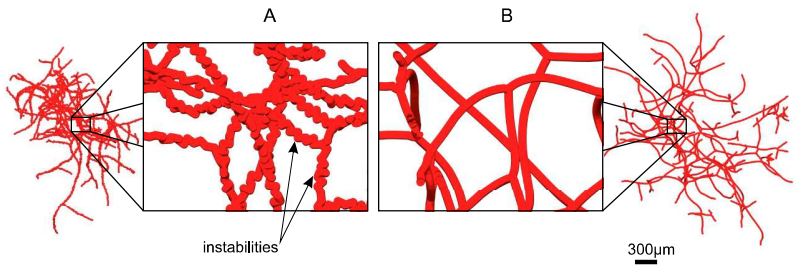

Figure S.5. Angular persistence forces stabilise vascular networks. (A) If the angular persistence force is inactive ($\lambda_{S_a} = 0$), then the network develops small-scale buckling instabilities that resemble the tortuous structures that characterise many solid tumours. **(B)** When the angular persistence force is included, the resulting vascular networks are smooth. Parameter values: as per Table S.1, except $\chi = 0.0$. Typical simulation results are plotted at time $t = 900$ ts.

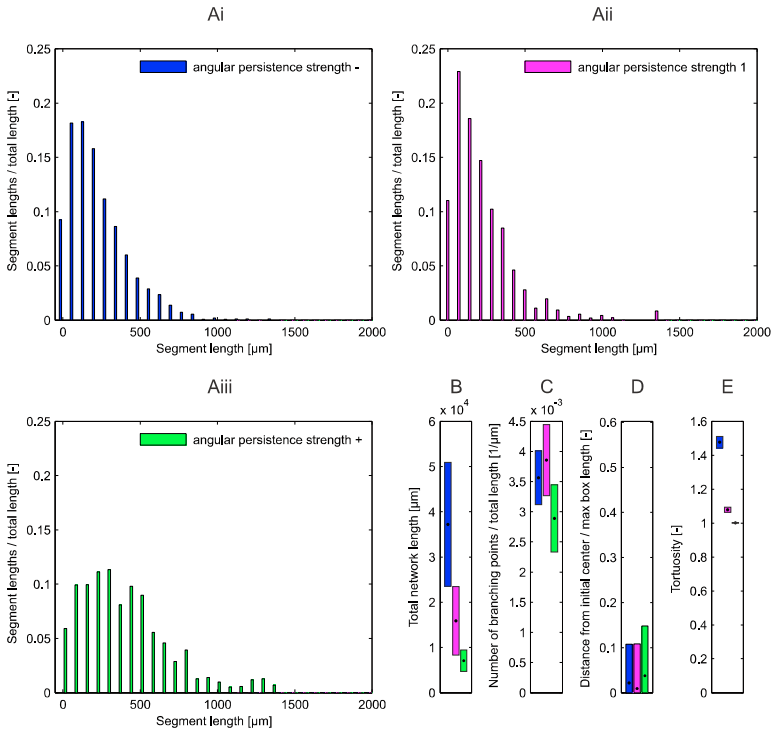

Figure S.6. Summary statistics showing how the vessel structure at time $t = 900\,\mathrm{ts}$ depends on the strength of the angular persistence force. Parameter sensitivity analysis shows how increasing the strength of the angular persistence force, ω_a, alters the properties of the simulated vascular networks. **(Ai–iii)** The distribution of vessel lengths shifts towards longer vessel segments as the angular persistence force increases. **(B, C)** As they became less dense, the total length of the vessel networks and the number of branching points per unit length decrease. For each choice of parameter values, summary statistics were obtained by averaging over 70 simulations. Parameter values: as per Table S.1, except $\chi = 0$, $\omega_a = 5.56 \times 10^{-7}$ (blue), $\omega_a = 5.56 \times 10^{-5}$ (magenta), $\omega_a = 5.56 \times 10^{-3}$ (green).

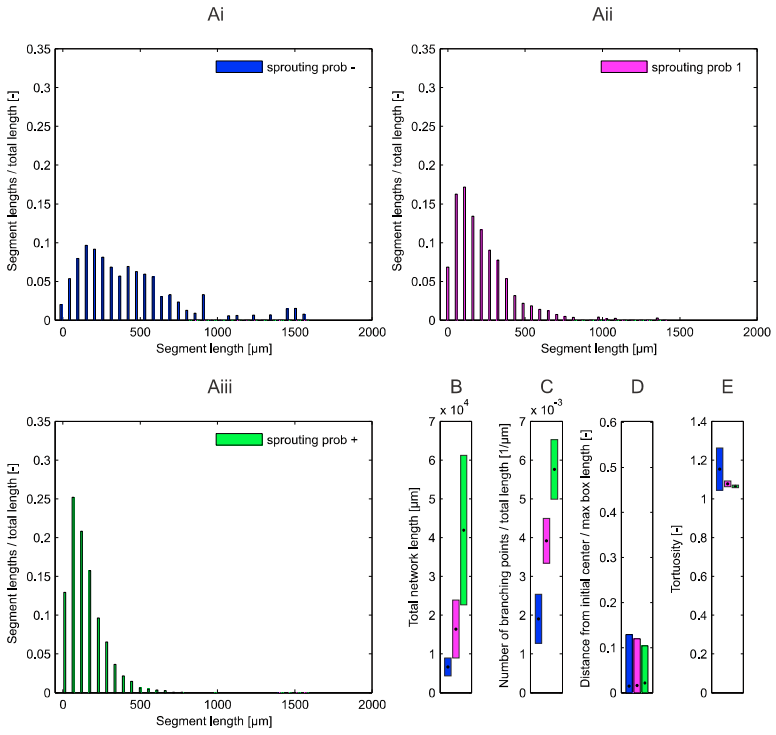

Figure S.7. Summary statistics showing how network structure at time $t = 900\,\text{ts}$ depends on the sprouting probability. The figure shows **(Ai–iii)** the distribution of vessel lengths, **(B)** the total network length, **(C)** the number of branches per unit vessel length, **(D)** the displacement of the centre of mass and **(E)** the tortuosity for different sprouting probabilities. The metrics which are most sensitive to variation in the sprouting probability are the total network length **(B)**, and the number of branch points per unit vessel length **(C)**. For each choice of parameter values, summary statistics were obtained by averaging over 70 simulations. Parameter values: as per Table S.1, except $\chi = 0$, $k_{\text{spr}} = 1.0 \times 10^{-4}$ (blue), $k_{\text{spr}} = 2.0 \times 10^{-4}$ (magenta), $k_{\text{spr}} = 3.0 \times 10^{-4}$ (green).